Michel Crucifix · Christopher D. Hewitt

# Impact of vegetation changes on the dynamics of the atmosphere at the Last Glacial Maximum

**Abstract** Much work is under way to identify and quantify the feedbacks between vegetation and climate. Palaeoclimate modelling may provide a mean to address this problem by comparing simulations with proxy data. We have performed a series of four simulations of the Last Glacial Maximum (LGM, 21,000 years ago) using the climate model HadSM3, to test the sensitivity of climate to various changes in vegetation: a global change (according to a previously discussed simulation of the LGM with HadSM3 coupled to the dynamical vegetation model TRIFFID); a change only north of 35°N; a change only south of 35°N; and a variation in stomatal opening induced by the reduction in atmospheric $CO_2$ concentration. We focus mainly on the response of temperature, precipitation, and atmosphere dynamics. The response of continental temperature and precipitation mainly results from regional interactions with vegetation. In Eurasia, particularly Siberia and Tibet, the response of the biosphere substantially enhances the glacial cooling through a positive feedback loop between vegetation, temperature, and snow-cover. In central Africa, the decrease in tree fraction reduces the amount of precipitation. Stomatal opening is not seen to play a quantifiable role. The atmosphere dynamics, and more specifically the Asian summer monsoon system, are significantly altered by remote changes in vegetation: the cooling in Siberia and Tibet act in concert to shift the summer subtropical front southwards, weaken the easterly tropical jet and the momentum transport associated with it. By virtue of momentum conservation, these changes in the mid-troposphere circulation are associated with a slowing of the Asian summer monsoon surface flow. The pattern of moisture convergence is slightly altered, with moist convection weakening in the western tropical Pacific and strengthening north of Australia.

M. Crucifix (✉) · C. D. Hewitt
Met Office, Hadley Centre for Climate Prediction and Research,
FitzRoy Road, Exeter, Devon, EX1 3PB UK
E-mail: michel.crucifix@metoffice.gov.uk
Tel.: +44-1392-884105
Fax: +44-1392-885681

## 1 Introduction

A positive climate feedback loop implies that the response of one component of the system reinforces the cause that produced the initial response. A classic example is that of the Siberian boreal forest: a cooler climate reduces the forest cover, which leads to an increased surface albedo due to a greater exposure of snow on the ground, which in turn enhances the cooling (Otterman et al. 1984). Such mechanisms are the subject of many research efforts using models at present, as they may substantially enhance the response of the climate system to the increase in greenhouse gases in the future. However, it is necessary to confront the model results with past climatic data in order to ensure that the important processes are represented in a quantitatively satisfactory manner. A feedback could be considered as important and properly represented if it substantially improves the match between simulation and data.

The Last Glacial Maximum (LGM, 21,000 years ago) is a very attractive candidate for studying climatic feedbacks, for example feedbacks related to vegetation changes. The LGM climate was dramatically different from that of today, and it is recent enough to be reasonably well-documented through proxy climate records (palæodata).

Different approaches have been tested. Crowley and Baum (1997) and Wyputta and McAvaney (2001) compared atmosphere general circulation model simulations of the LGM using, in one case, a data-based reconstruction of the LGM vegetation and, as a comparison, a reconstruction of the modern vegetation. Both studies stressed the magnitude (6–10°C) of the Siberian cooling

resulting from the vegetation dieback in that region. Wyputta and McAvaney (2001) noticed a strengthening of winter continental highs, and a deepening of Aleutian and Icelandic lows. Crowley and Baum (1997) also described a decrease in precipitation caused by the reduction of the tropical rainforest. Kubatzki and Claussen (1998) adopted an iterative process using the ECHAM3 atmosphere model. LGM vegetation maps were obtained by successively running an equilibrium biosphere model with the outputs of ECHAM3. Such an approach presents a substantial advantage to that of Crowley and Baum (1997) and Wyputta and McAvaney (2001) because the vegetation map is consistent with the simulated climate. In particular, by starting the iterative process from different initial conditions, they could verify the presence of several stable states for the climate-vegetation system at the LGM. They also reported a connection between reduced rainfall in the Sahel (caused by regional changes in vegetation) and convection over the Indian sub-continent. The next step has been to use an interactive, dynamical vegetation component that is then considered as an integral part of the climate model (Levis et al. 1999). The latter class of models maximises the consistency of the relationships between surface fluxes, vegetation growth and maintenance, and atmosphere dynamics.

The European MOTIF project (Model and Observations to Test clImatic Feedbacks, http://www-lsce.cea.fr/motif) will pursue these efforts and quantify vegetation and ocean feedbacks for the periods of the LGM and the mid-Holocene (6 kyear BP). The modelling part of MOTIF comprises a series of simulations performed with state-of-the-art climate models (usually more complex than above, including ocean dynamics and having a higher resolution) coupled with dynamical vegetation models. MOTIF partners are also part of the broader PMIP 2 project (Palaeoclimate Modelling Intercomparison Project 2, http://www-lsce.cea.fr/pmip2, see also Harrison et al. 2002).

However, the increase in the number of degrees of freedom that accompanies the evolution towards more complex models may pose problems. For example, calculated vegetation sometimes deviates from the observed or reconstructed one. As a consequence, the calculated feedback may be wrong locally. We want, in that case, to be able to extract information that is relevant at the global scale, even if some processes are misrepresented at the local scale. Another difficulty is linked to the many possible interactions and teleconnections operating in ocean–atmosphere models. They could be disentangled with additional sensitivity studies, but the computing resources to run such models are often tight. Therefore, the inter-comparison of MOTIF and PMIP II experiments must be complemented by experiments with more idealised set-ups.

Here, we analyse a series of "atmosphere-slab ocean" experiments, for which the ocean is represented by a 50-m-deep layer of water with prescribed, seasonally varying, heat fluxes. The main drawbacks of using a slab model are a less realistic representation of inter-annual variability and some locally important errors (Hewitt et al. 2003), when calculating the response of sea-surface temperature to changes in boundary conditions. The advantage is a substantial reduction in the computing cost because the required simulation length is much shorter. It is therefore an ideal set-up to give a preliminary answer to five questions that we have chosen to focus on:

1. What are the impacts of vegetation changes on the energy balance of the system?
2. What are the consequences for the atmosphere dynamics?
3. Can vegetation changes in one location influence climate (and perhaps vegetation) somewhere else?
4. Can we infer general conclusions about the impact of changes in tropical rainforest on climate?
5. How will our results guide us in future experiment designs and analyses?

## 2 Experimental setup

### 2.1 Model and boundary conditions

We used HadSM3, the slab-ocean version of the third generation Hadley Centre Climate Model (Hewitt et al. 2001). It is coupled to the latest Met Office Surface Exchange Scheme, MOSES II (Essery et al. 2003). The ocean is represented by a 50-m-deep "slab" of water with prescribed spatially and seasonally varying heat fluxes calculated to give realistic sea-surface temperatures (Rayner et al. 1996) under pre-industrial forcing.

On each grid point of the continent, MOSES II represents the land surface as a mixture of up to five plant functional types (broadleaved trees, needleleaved trees, C3 grass, C4 grass and shrubs), plus bare soil, inland water, continental ice and urban surface. Surface albedos are specified as single values for all short-wave bands. The distribution maps for bare soil albedo and soil texture are taken from Wilson and Henderson-Sellers (1985). Fresh, deep-snow albedo depends on the underlying surface type: 0.3 on trees, 0.4 on shrubs, 0.6 on grass and 0.8 on bare soil. Soil hydrological and thermic properties depend on the soil texture according to a lookup table given in Cox et al. (1999). Soil moisture and temperature are derived from a soil model with four layers in the vertical. Vegetation evapotranspiration is calculated consistently with the net primary productivity, itself derived from a leaf photosynthesis model (Cox et al. 1998). The surface radiative balance and the turbulent fluxes that are transmitted to the boundary layer scheme are calculated separately over each surface type.

The atmospheric component (HadAM3, resolution of $3.75° \times 2.50° \times 19$ layers on the vertical) has proved to provide a good representation of the tropical and extratropical dynamics, including aspects linked to

precipitation distribution and variability at both intra-seasonal and inter-annual time scales (Inness et al. 2001; Pope and Stratton 2002). The main discrepancies relevant to our purpose are a tendency to underestimate surface temperature in descent areas (Pope et al. 2000) and, specific to this version using MOSES II, to underestimate monsoon convective rainfall in Sahel and India. More specific validations of the slab-ice component and the MOSES II surface scheme are available in Hewitt et al. (2001) and Essery et al. (2003), respectively.

Two experiments performed with HadSM3 coupled to the TRIFFID (Cox et al. 2001) dynamical vegetation model analysed in Crucifix et al. (2005a), hereafter C05, serve as the starting point of the present study. One experiment (called PI-289 in C05) provides a representation of the pre-industrial climate; the other one (LGM_207) is for the LGM. These two simulations used interactive vegetation. They were continued for 30 years, keeping the same mean distribution of vegetation fraction, leaf-area-indices and canopy height (these are detailed in Fig. 1). The main modification with respect to the original experiments is the suppression of inter-annual and intra-annual variability in vegetation structure, but this does not change the mean climate significantly. These two experiments are further referred to as PI_VPI (the experiment uses Pre-Industrial climate boundary conditions and Pre-Industrial Vegetation) and LGM_VLGM (LGM climate boundary conditions with LGM vegetation). To these are added four sensitivity experiments as follows:

– LGM_VPI: uses climate boundary conditions of the LGM, but the vegetation map of PI_VPI;
– LGM_VLGMH: as LGM_VPI but uses the LGM vegetation map north of $35°N$, and the pre-industrial potential vegetation map south of this boundary;
– LGM_VLGMT: as LGM_VPI but uses the LGM vegetation map south of $35°N$, and the pre-industrial potential vegetation map north of this boundary;
– LGM_VLGM289: as LGM_VLGM, but uses the pre-industrial concentration of $CO_2$ (289 ppmv) in the plant physiology equations.

Comparing LGM_VPI with LGM_VLGM tells us about the contribution of vegetation changes to climate changes between the LGM and the pre-industrial climates. The difference LGM_VLGM–LGM_VPI corresponds to the term $\Delta V$ in feedback analysis theory (Berger 2001; see Ganopolski et al. 1998; Crucifix and Loutre 2002 for applications). LGM_LGMH and LGM_LGMT allow us to isolate the effects of northern extratropical vegetation from the tropical one and highlight possible connections between vegetation changes in one region and the response of the atmosphere in another region. LGM_VLGM289 will help us to determine whether, vegetation structure being equal, the increase in stomatal opening caused by the reduced $CO_2$, has a significant impact on atmosphere dynamics

Fig. 1 Simulated potential distribution of plant function types for the pre-industrial and the Last Glacial maximum using HadSM3_TRIFFID. These maps serve as boundary conditions in the present study. A full analysis is available in Crucifix et al. (2005a). We recall the main features. For the pre-industrial, the main discrepancies with respect to the reconstructions are: overestimated poleward extension of tropical rainforest, insufficient poleward advance of needle-leaved trees (northern taiga is represented by shrubs) and quasi-absence of shrubs in semi-arid areas; for the Last Glacial maximum, the model correctly reproduces the dieback of the taiga, the extension of subtropical deserts and the reduction in tree-cover in equatorial areas. The tree cover remains overestimated in sub-equatorial zones (especially in Amazonian) as well as in Europe
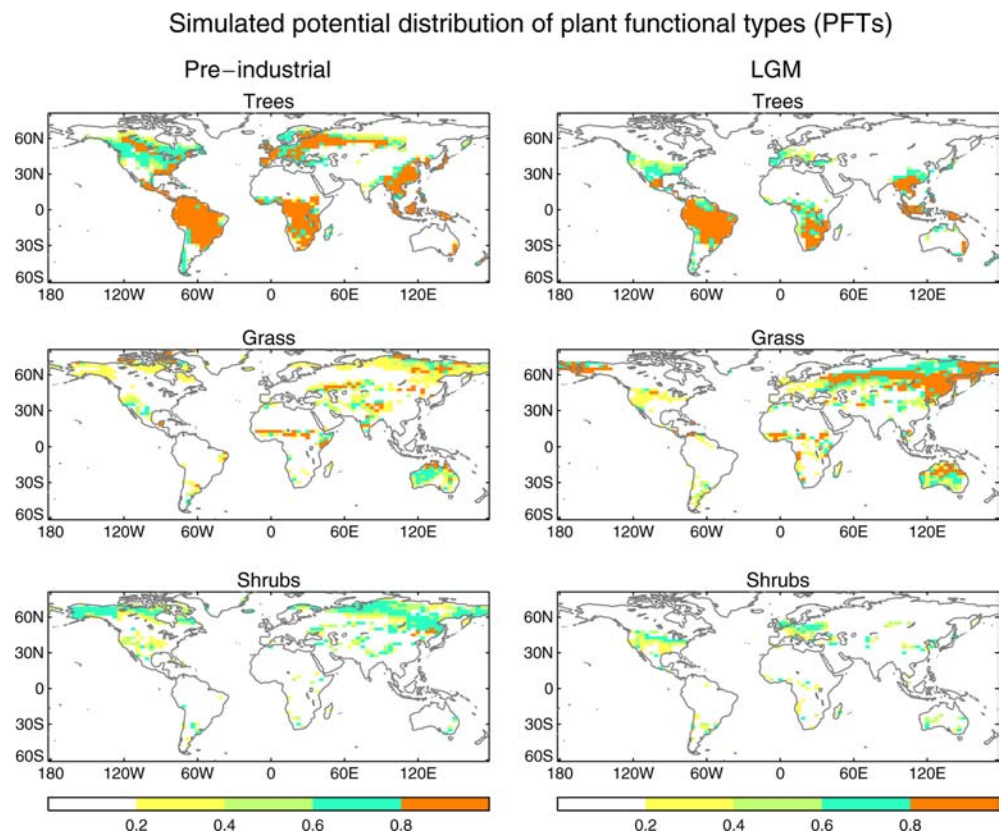
or not. All LGM experiments use a $CO_2$ concentration of 207 ppmv for the atmospheric radiative calculations, Peltier's (1994) ICE-4G reconstruction of topography and ice-sheet extent, a sea-level lowered by 105 m with respect to today, and Berger's (1978) calculation of top-of-the-atmosphere insolation 21,000 years ago.

## 3 Impact of vegetation changes on surface temperature

Figure 2 displays a series of annual mean surface temperature differences. The upper-left panel shows the LGM_VLGM–PI_VPI difference. This signal includes the vegetation feedback. It is seen that continental temperatures are colder almost everywhere at the LGM than at the pre-industrial, with the difference increasing from the south to the north. The differences are largest (exceeding 20°C cooling) over the ice sheets. However, there is some warming larger than 2°C in India and some parts of Sub-Saharan Africa. The topright graph shows the LGM_VLGM–LGM_VPI difference. This is the contribution of vegetation change to the total difference. The vegetation changes prove to contribute greatly to the total signal in a number of places: Russia (8°C cooling), where trees are replaced by tundra; Tibet (10°C cooling) where grassland is replaced by bare soil; and the cited semi-arid areas (2°C warming), where grasslands are replaced by bare soil. The apparently incoherent

effects of replacing grass with bare soil are explained in the next paragraph. There is also a cooling at the southern edge of the Laurentide ice sheet, although the contribution there is small with respect to the total signal. The two lower graphs provide the separate contributions of vegetation north and south of 35°N. It is seen that the temperature response is located where the vegetation change actually occurs. However, in global mean, there is a synergy between the two zones: the total globally averaged contribution of vegetation changes (−0.6°C) is larger than the sum of the zonal contributions (−0.3°C). This synergy materialises at two places: (1) in the Arctic sea-ice: the Arctic is colder when vegetation changes are taken into account everywhere; and (2) in Tibet, where the cooling initially caused by the local vegetation change is strengthened (by 1°C) when both mid- and high-latitude vegetation changes are taken into account.

The origin of continental temperature changes can be traced back with the help of Fig. 3, which describes the contribution of various terms (clear-sky short-wave balance, top-of-the-atmosphere cloud forcing, surface sensible and latent heat), with warm colours (yellow–red) indicating a contribution to warming. It is seen in the top left graph that both Siberian and Tibetan coolings are to be related with an increase in albedo (less absorbed short-wave radiation). The top right plot of Fig. 3 shows that the magnitude of the
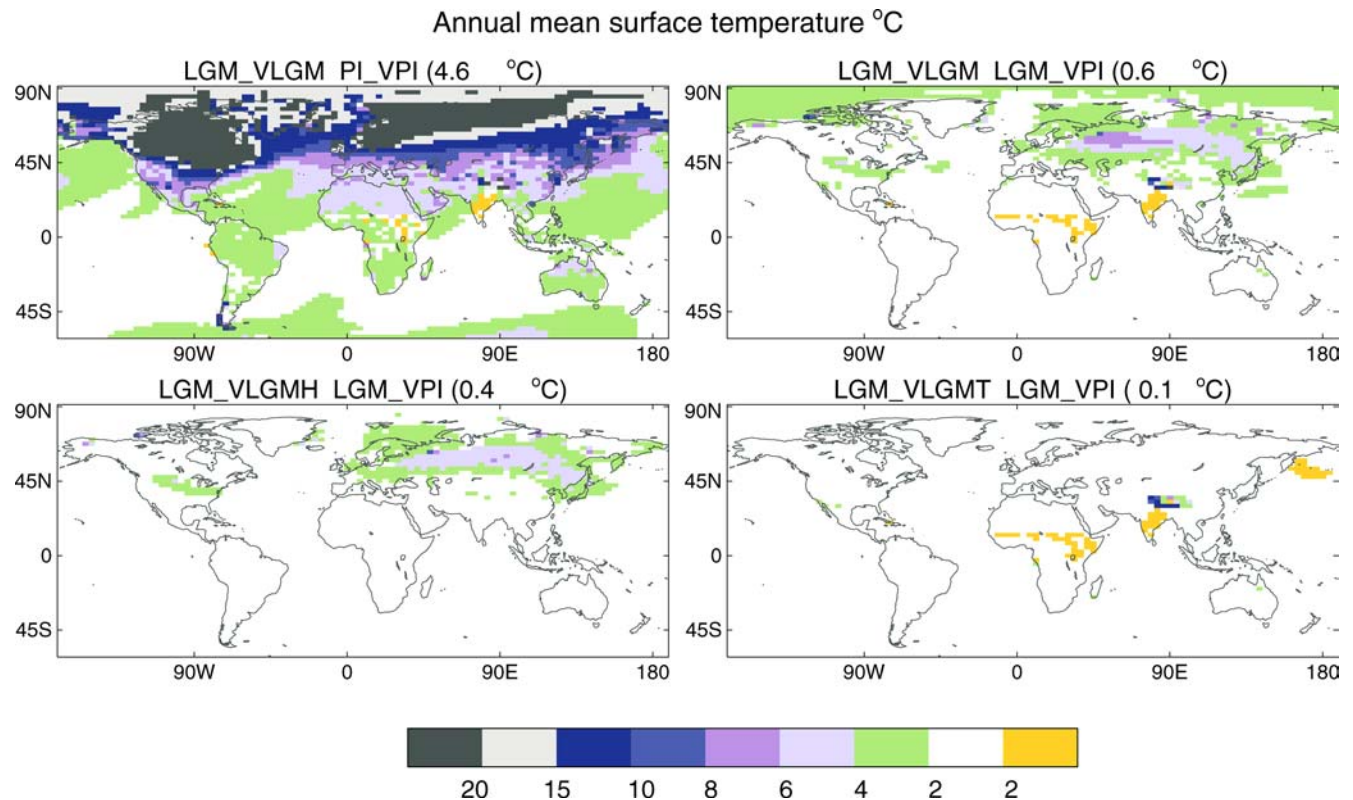


Fig. 2 Surface temperature differences: *top left*: total change between LGM and the pre-industrial epoch; *top right*: total contribution of vegetation changes; *bottom left*: contribution of vegetation north of 35°N and *bottom right*: contribution of vegetation south of 35°N. *Values between parentheses* are the global means
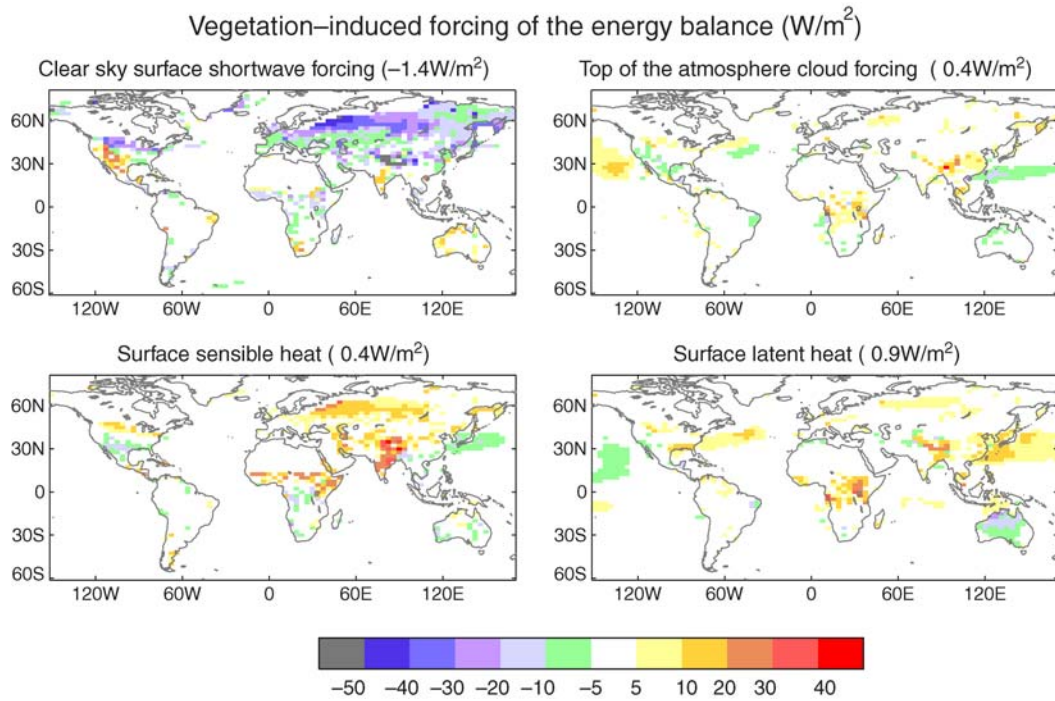
**Fig. 3** Annual mean vegetation forcing of the different terms of the atmosphere energy balance, calculated as the difference between simulations LGM_VLGM and LGM_VPI. Fluxes are downwards positive, i.e. a positive value is associated with a surface warming. *Values between parentheses* are global means

**Fig. 4** Seasonal cycles of grid-box mean albedo and snow fraction in the different experiments for two locations representative of the West Siberian Plains (*top*) and the Plateau of Tibet (*bottom*)
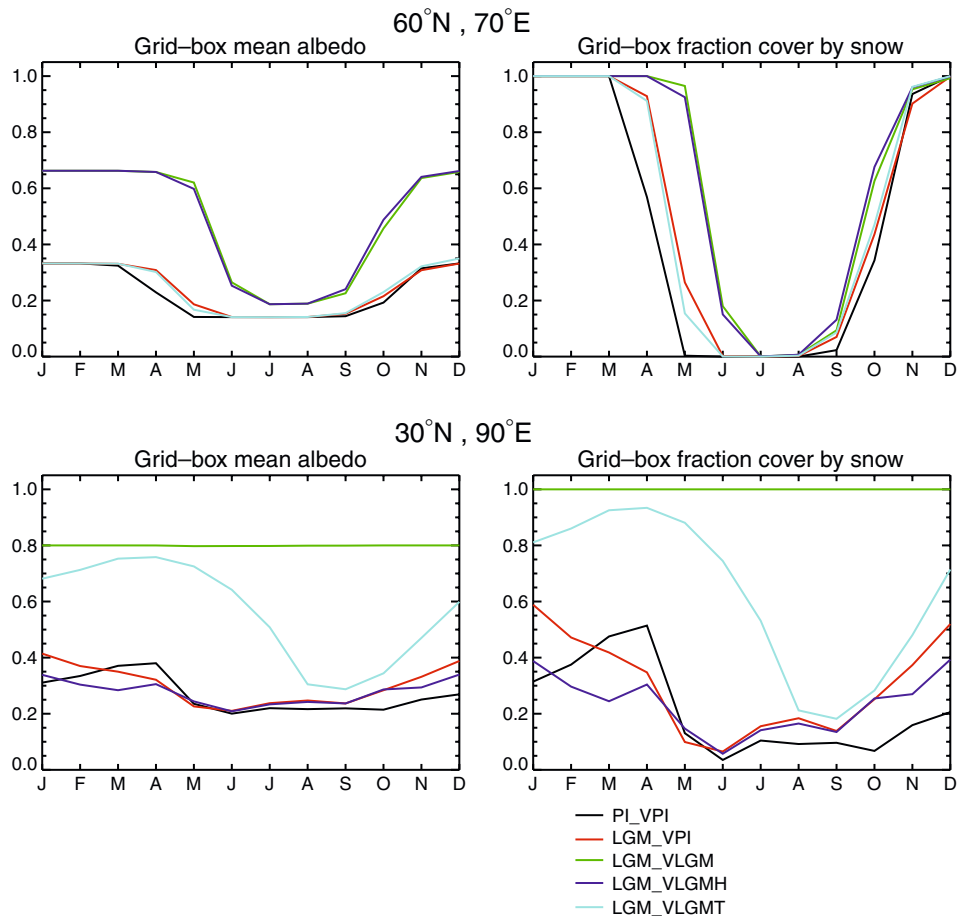
top-of-the-atmosphere cloud radiative feedback (total clear-sky radiation minus all-sky outgoing radiation) is small. A detailed analysis for short-wave and long-wave radiation shows that there is a decrease in convective cloud cover—especially in central Africa—but that the effects on short-wave and long-wave cloud forcings compensate each other. The warming seen in semi-arid areas is related to a decrease in sensible heat exchange between the surface and the boundary layer (bottom left graph): this is a consequence of reduced roughness length. In the African rainforest, reduced evapotranspiration (bottom right graph) could potentially have driven a warming (as observed by Crowley and Baum 1997), but it can be seen in Fig. 2 that the impact on surface temperature is less than 2°C.

How does vegetation affect albedo changes between the LGM and today? In Siberia, the phenomenon is well known (Otterman et al. 1984): the disappearance of forest results in an increase in albedo during the snow season. The effect is depicted in Fig. 4: the top left graph shows the grid-box mean albedo at 60°N, 70°E, where trees have been replaced by a mixture of grass and bare soil. Winter and spring albedo are around 0.35 in the modern-vegetation experiments (black, red and light blue); it is around 0.65 in the LGM vegetation experiments (green and dark blue). The top right graph shows the seasonal cycle of snow fraction. With modern vegetation, the LGM climate (red curve) has a snow-season length of about 1.5 months longer than at the pre-industrial (black curve). Including LGM vegetation (green curve) further lengthens the snow-season by another 1.5 months. This synergy between snow and vegetation was earlier described with a model of intermediate complexity (Crucifix and Loutre 2002). In Tibet, the albedo increase is initially related to the shift from grass to bare soil (snow-covered grass is assumed to have an albedo 0.2 less than snow-covered bare soil in this version of the model). However, as seen on the
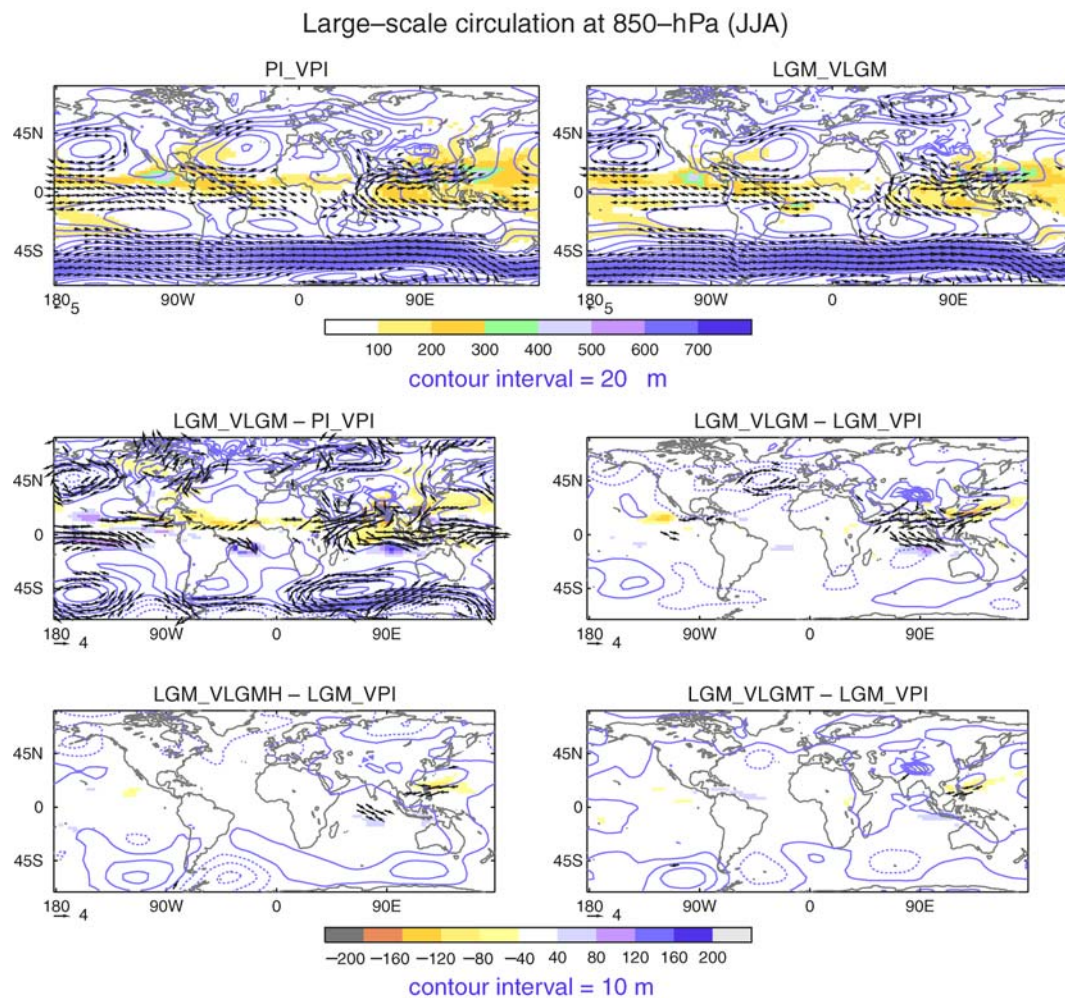


Fig. 5 Low-level large-scale circulation for JJA at the pre-industrial and the LGM (*top*), plus a series of differences between the various experiments. The *colours* represent the rate of latent heat released by convective precipitation (W/m²). *Contours* are the geopotential at 850 hPa (*negative values are dotted*), and *arrows* are the wind for the same level (absolute values less than 5 m/s and differences less than 2 m/s are not plotted)

bottom right panel of Fig. 4, this small effect is strongly amplified by an increase in the snow fraction: compare the red curve (no vegetation change) with the light-blue curve (vegetation changes south of 35°N). Furthermore, the fraction is further increased when vegetation change in Siberia is taken into account (green curve).

One conclusion of the present analysis is that a change in vegetation in different regions may have opposite effects on temperature, depending on the environment. When there is snow, reducing vegetation height causes an increase in albedo, thus a cooling. This effect has been assessed with independent models of various levels of sophistication (Harvey 1988; Bonan et al. 1992; Crowley and Baum 1997; Kubatzki and Claussen 1998; Viterbo and Betts 1999; Wyputta and McAvaney 2001), which our results for Siberia are in quantitative agreement with. In semi-arid areas, the effect of vegetation, in this model, is mainly seen through changes in turbulent exchanges of latent and sensible heat. This is consistent with an earlier analysis of inter-annual variability in HadSM3_TRIFFID (Crucifix et al. 2005b); where we indicate that a

decrease in vegetation cover in semi-arid areas reduces both evapotranspiration and sensible heat exchanges, although the impact on boundary layer temperature was not always found significant. Other models (Zhang and Henderson-Sellers 1996; Kubatzki and Claussen 1998) suggest an impact of the cloud response on the energy balance of the climate system of same sign and similar amplitude as the one described here. The very different natures of the experimental set-ups prevent us from pushing the model inter-comparison much further at this stage.

## 4 Understanding the consequences of vegetation changes on atmosphere dynamics

The absolute values and differences between the various experiments in geopotential heights at 200, 250 and 850 hPa, vertical velocity, surface pressure, long-wave cloud forcing and vertical cross-sections of zonal wind and air temperature, were examined for each month and each season of the year. The features estimated to be the
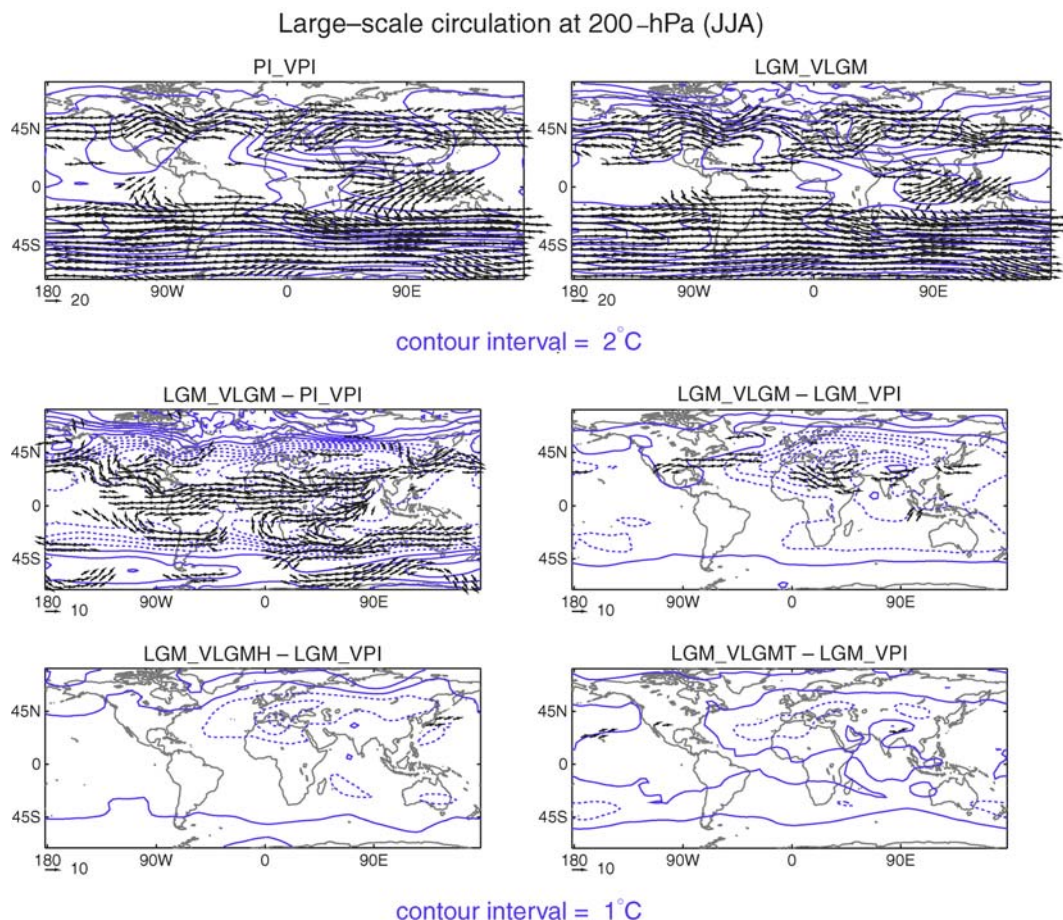


**Fig. 6** Upper-troposphere large-scale circulation for JJA at the pre-industrial and the LGM (*top*), plus a series of differences between the variou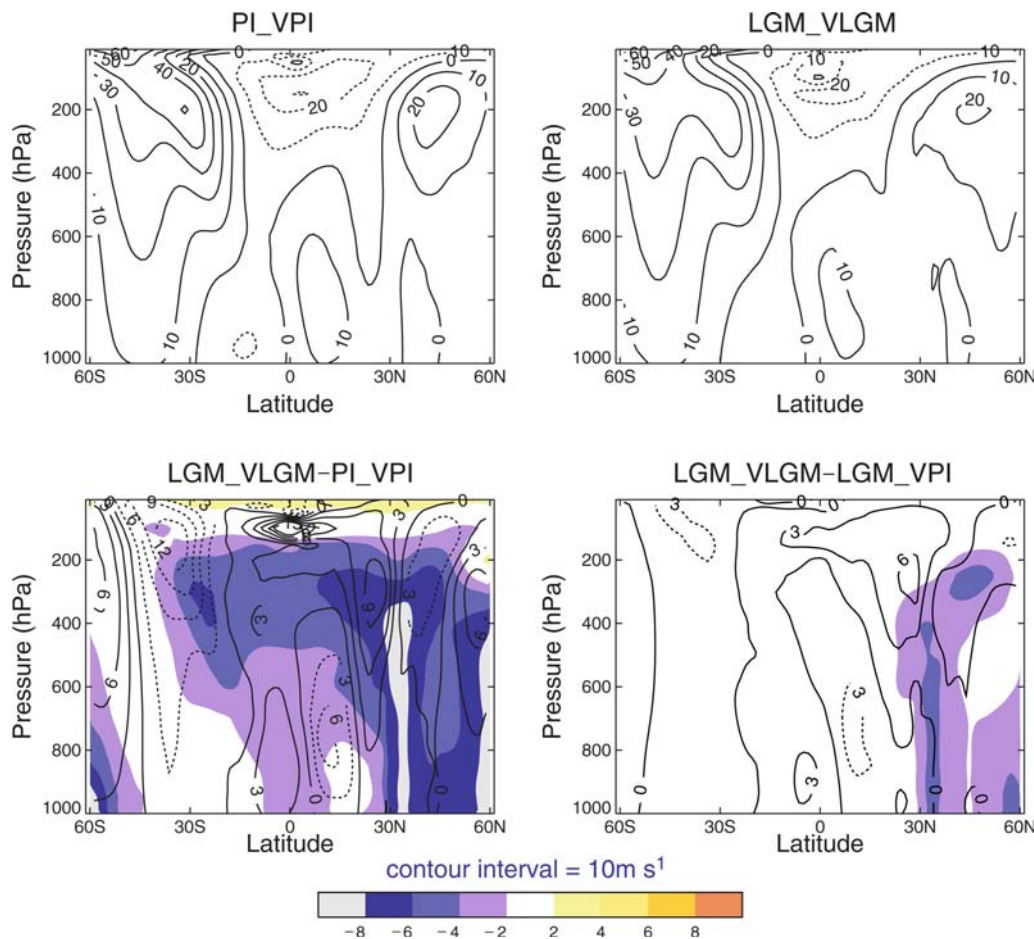s experiments. *Contours* are the temperatures at 200 hPa (*negative differences are dotted*), and *arrows* the wind for the same level (absolute values less than 10 m/s and differences less than 5 m/s are not plotted)

most meaningful are observed in June–July–August (JJA). They are described here.

Figure 5 displays, for a number of situations, the position and strength of the low-level jets (850 hPa, arrows), the 850-hPa geopotential height (blue contours) and the latent heat released by convective precipitation (colour scale). The two upper graphs are the simulated mean climatologies for pre-industrial and LGM averaged over JJA. Classical features of summer circulation can be recognised, such as the tropical anticyclones, the North Atlantic one extending over the Mediterranean region; the summer low-level flows characterising the summer Asian monsoon, including easterly trade winds south of the equator, the Somali jet and the westerly jet over India; the centres of convection in the Bay of Bengal, China Sea and to the west of the Mexican coast; the Atlantic and Pacific trade winds, and finally the Antarctic circumpolar winds. The two middle graphs describe the total changes between LGM and pre-industrial (left) and the contribution of vegetation (right). The essential features of the summer circulation changes between LGM and pre-industrial are an overall reduction of the convective activity, especially in the

Atlantic-Africa Intertropical convergence zone and in the Asian monsoon complex, a slowing of the Asian monsoon flow, and a decrease in the Pacific trade winds' intensity. Among these features, the main effect of the vegetation changes is to slow-down the Asian monsoon flow, with convection decreasing downstream of the monsoon flow and strengthening upstream of it. This response is also associated with a slight weakening of the Azores Anticyclone. The two lower graphs provide the separate contributions of northern extratropical vegetation (left) and those of the remainder of the world (right). This figure shows that the impacts of these changes are similar but weaker than the total contribution of vegetation. Therefore, it can be concluded that high-latitude and low-latitude vegetation changes act in concert to produce a significant alteration in Asian monsoon dynamics.

In order to understand the connection between vegetation changes and the slow down of the monsoon, it is necessary to examine several aspects of the upper-troposphere circulation. Figure 6 shows the strength and position of the tropospheric jets at 200 hPa (arrows) and temperature for the same level (contours). As for Fig. 5,



Fig. 7 Meridional cross sections (zonal average between 70° and 100° longitude). *Upper graphs* show the zonal winds in the pre-industrial and LGM experiments. The *lower graphs* show differences in temperature (*colours*) and zonal wind (*contours*)

the two upper graphs show the simulated pre-industrial and LGM summer climates. The main features seen here are the subtropical front around 45°N, the westerly jet slightly north of this front, and the easterly jet from India to Africa north of the equator. The simulated LGM climate reveals a slightly different structure for the subtropical front, which is less zonal and passes across the Mediterranean sea. We attribute this change to the enhanced thermal contrast at the surface between northern Eurasia and Europe on the one hand, and the Eurasian tropical deserts on the other hand. The two middle graphs show the total difference between the LGM and the pre-industrial epoch (left), and the contribution of vegetation (right). The contribution of vegetation is manifested through (1) a south-eastwards shift of the subtropical front, resulting in a substantial tropospheric cooling around 40°N between approximately 10°W and 120°E with a maximum over the Mediterranean, and (2) a weakening of the tropical easterly jet, materialised by westwards anomalies over Eastern Africa, Arabia and India. Similar mid-troposphere temperature differences can also be observed when only part of the vegetation changes are taken into account, as shown in the two bottom graphs of Fig. 6. The total contribution of vegetation is roughly the sum of the partial contributions.

Temperature and wind cross-sections (Fig. 7) help us to analyse the consequences of this shift of the subtropical front on the vertical structure of the atmosphere. The two top graphs give the mean JJA zonal wind for pre-industrial and LGM. One can recognise, from south to north, the Southern westerlies, the low-level monsoon easterlies (mainly seen in the pre-industrial), the tropical easterly jet (around 200 hPa) and the northern mid-latitude westerlies. With respect to the pre-industrial, the LGM exhibits a weaker tropical easterly jet. The bottom graphs (contours) show wind differences between pairs of experiments. The left graph is the LGM minus the pre-industrial, and the right graph is the contribution of vegetation. It is seen that the vegetation changes reduce the velocity of the tropical easterly jet by about 3 m/s (roughly 15%). Superimposed on the contours are the differences in atmosphere temperature. The link between wind and temperature imposed by the thermal wind relationship can be recognised. The decrease in the velocity of the easterly jet is caused by a cooling north of the easterly jet. Vegetation changes contribute to this cooling, essentially around the Tibetan plateau (30°N) and through the southward shift of the subtropical front (40°N, around 300 hPa).

The next step is to understand the connection between the intensity of the jet and the surface circulation features. This can be done by analysing the meridional transport of momentum during JJA shown in Fig. 8. The zone that interests us is where momentum is transported northward by the Hadley Cells, between 20°S and 20°N. It is seen that the transport at the LGM is smaller than at the pre-industrial. Furthermore, vegetation accounts for about half of the reduction, because the magnitude of the northward transport of momentum in the summer tropics is linked to the intensity of the easterly jet. The experiments where only part of the vegetation changes are prescribed have a transport intermediate between full vegetation change and no vegetation change. Momentum conservation imposes a corresponding reduction in surface drag, and hence, a weakening of the Hadley Cell surface features, including the Asian summer monsoon.

In summary, Siberian and Tibetan vegetation changes increase the albedo of the snow field. This effect is amplified by a lengthening of the snow season. The resulting surface coolings push the subtropical front southwards which, because of the thermal wind relationship, reduces the intensity of the subtropical easterly

**Fig. 8** Total zonal meridional transport of momentum in the different experiments presented in this study



Meridional transport of momentum : JJA ($10^{12}$ kg m$^2$s$^{-2}$)
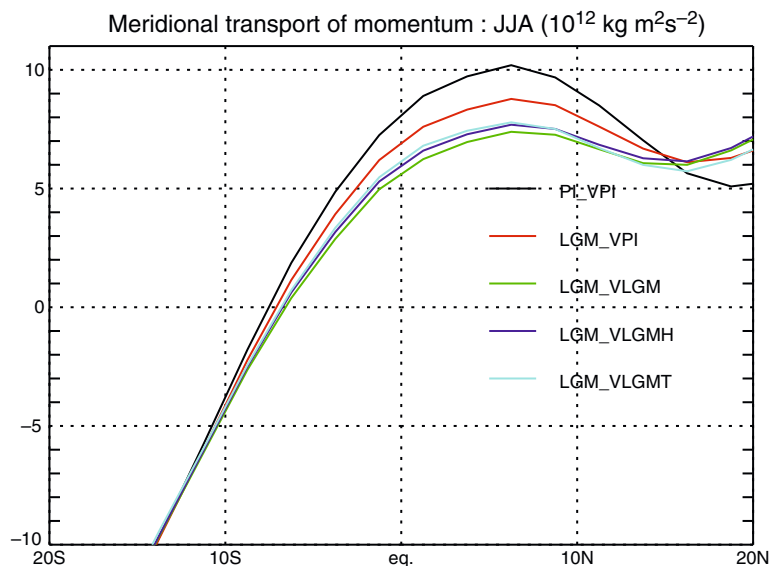
jet. Momentum conservation implies that this decrease is compensated for by a weakening of the low-level circulation. The pattern of moisture transport is therefore affected, resulting in more convection upstream of the monsoon low-level flow, and its less convection downstream. This new equilibrium also implies a rebalancing of sea-level pressure ($+12$ hPa in Tibet; $+3$ hPa in northern subtropical, western Pacific; $-1$ hPa in southern sub-tropical Indian; values given for JJA).

Relationships between Eurasian snow-cover and summer monsoon activity have long been observed. Present-day observations support Blanford's (1884) proposal that above-normal winter-snow fall in Eurasia, especially in the Himalayas, are followed the next summer by poor monsoon (Hahn and Shukla 1976; Dickson 1984). More recently, Zhang et al. (2004) documented, in NCEP re-analyses, a significant anti-correlation at the inter-decadal time-scale between increasing Eurasian snow-cover and decreasing precipitation in Eastern-Asia/South-East China. The mechanisms underlying this connection have been studied with climate and weather forecast models (Barnett et al. 1989; Yasunari et al. 1991; Vernekar et al. 1995; Bamzai and Marx 2000; Becker et al. 2001). Simulations consistently show that above-normal Eurasian snow-cover is associated with weaker-than-normal summer monsoon dynamics (weaker easterly jet, surface stress and geopotential through over India), although Becker et al. (2001) con-sider that the practical importance for seasonal forecast is limited. Two fundamental consequences of above-normal snow-cover are usually underlined (Barnett et al. 1989; Yasunari et al. 1991): in spring, the high albedo of snow reduces absorption of heat by the atmospheric column ("albedo effect"); in summer, snow melt prevents the surface from warming ("hydrological effect"). The subsequent cold anomaly over Tibet has a negative impact on the meridional northward temperature gradient in summer and on the latent heat released in the atmospheric column. Feedbacks of the ocean may also be involved (Barnett et al. 1989). Note that the albedo term largely dominates in our study of the LGM (Fig. 3). Snow melt is actually smaller in the experiment with LGM vegetation. A third effect is mentioned by Yasunari et al. (1991) and Bamzai and Marx (2000): increased snow-cover and soil-moisture cause an increase in evaporation. Yasunari et al. (1991) argue that this may favour convective events, thereby counteracting the albedo and hydrological effects. Zhang et al. (2004) also present evidence that increased evaporation may feed the formation of quasi-stationary eddies and subsequent precipitation East of Tibet. Clearly, increased evaporation is not observed in our simulation of the LGM (like snow-melt, evaporation is lower with glacial vegetation). This is not surprising because the glacial climate is much colder and dryer than the present-day. We therefore show results that are overall consistent with studies focusing on present-day variability in Asian
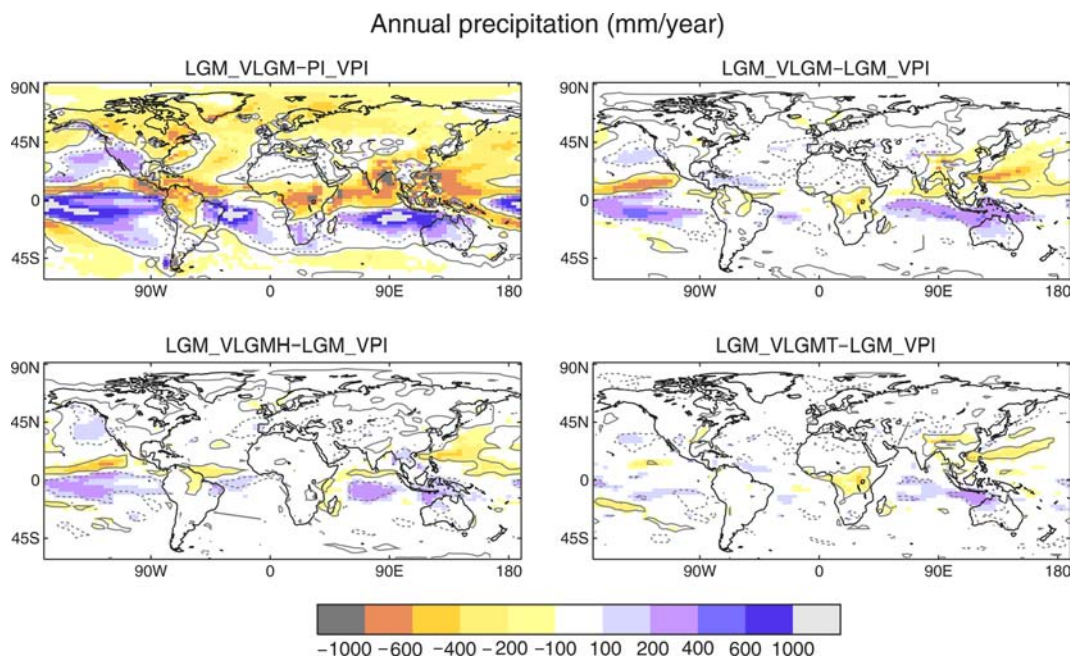


**Fig. 9** Total, annual precipitation: *top left*: total change between LGM and the pre-industrial epoch; *top right*: total contribution of vegetation changes; *bottom left* contribution of vegetation north of 35°N and *bottom right*: contribution of vegetation south of 35°N. Overplot are the 0.05 (*full line*)—0.95 (*dashed-line*) confidence interval with the null-hypothesis that mean precipitation is the same in the two experiments. In other words, areas in the *dashed-line-contour* have confidently more precipitation and areas in the *full-line-contour* have confidently less precipitation. Confidence levels are obtained from a T-test, assuming no spatial nor inter-annual correlation, which tends to underestimate the non-rejection interval

monsoon, be we suggest that the relative importance of the different mechanisms by which this connection between Eurasian snow-cover and South-Asian monsoon occurs, may have been different in a glacial climate. Interestingly, Bush (2002) focused on the Asian monsoon at the LGM on the basis of short integrations with an ocean–atmosphere GCM. He reported an almost doubling of the strength of the summer Indian westerlies at the LGM with respect to the pre-industrial, and he attributed this to the increase in Himalaya snow-cover. This result is opposite to ours. It is difficult to trace back the origin of these diverging conclusions, but the shift of the subtropical front observed in our experiments is an important aspect of the linkage between low and high-latitudes.

A few studies have specifically focused on the teleconnections related to vegetation changes. Xue and Shukla (1996) and Kubatzki and Claussen (1998) documented a link between tropical vegetation changes and the tropical easterly jet, although the mechanism was related to Sahara/Sahel land-surface properties. Earlier, we noted a contribution of vegetation in reducing the strength of the Azores anticyclone. This feature is not very persistent from one experiment to the next and it might be an artefact due to inter-annual variability. For example, it is not seen when only partial vegetation changes are accounted for. We note, however, that Rodwell and Hoskins (2001) have argued for connections between summer convection in Asia and the strength of subtropical anticyclones. Our results would therefore be consistent with their findings. It is noteworthy that the response of atmosphere dynamics over Sahel is small in our model. This contradicts the findings by Kubatzki and Claussen (1998). This is because in the glacial climate of our model, Sahel is North of the zone influenced by the African monsoon. Therefore, a change in Sahel surface properties has little consequences for large scale atmosphere dynamics.
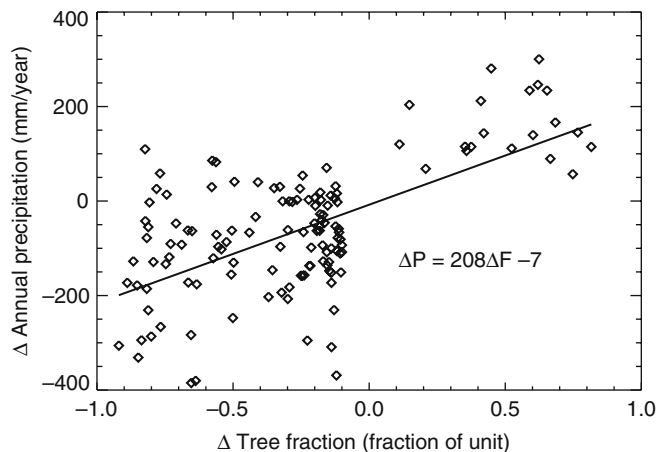


**Fig. 10** Scatter plot and regression line between the response of precipitation between 20°S and 20°N to vegetation change, and the variation in tree fraction

Finally, the deepening of the winter Aleutian low in response to imposing glacial vegetation, reported by Wyputta and McAvaney (2001) can briefly be commented on. We observe a winter cyclonic anomaly centred around 40°N in the Pacific ocean. The amplitude of the anomaly on the 500 hPa-geopotential height is 30 m. The amplitude and location are therefore in quantitative agreement with Wyputta and McAvaney (2001). However, the cyclonic anomaly is, in our case, located South of the Aleutian low. The Aleutian low itself is actually slightly weakened.

## 5 Response of precipitation

Figure 9 displays the response of annual precipitation to the total LGM forcing, including the vegetation feedback (top left) and the contribution of vegetation only (top right). The two lower graphs display the partial contributions of vegetation (northern vegetation on the left, tropical and southern vegetation on the right). The impact of vegetation changes is relatively small with respect to the total change. On the other hand, local responses can be distinguished from remote ones. The local responses are observed on the tropical continents in the bottom right panel. They consist of a reduction in convective rainfall in Africa and the south-west of Tibet. In Africa, this response is likely to be related to a decrease in evapotranspiration, which reduces the likelihood or the strength of moist convective precipitation events. This feedback was earlier described by Eltahir (1996), except that, in our case, there is no clear response of the large-scale convergence. South-west of Tibet, convection is inhibited by cold winds blowing from the Tibetan plateau. The phenomenon is amplified by a reduction in large-scale precipitation. The remote responses are observed in the Indian and Pacific oceans, including part of northern Australia. They appear even if vegetation is only partly changed, and the partial contributions add up roughly linearly to form the total contribution of vegetation. The observed pattern is consistent with the discussed reduction in summer Hadley Cell activity. It is amplified by slight inhibition in winter, of the convective activity north of the equator, which benefits moisture convergence and convection downstream of the winter monsoon surface flows.

The absence of a response of precipitation to vegetation changes in Amazonia is not surprising because the changes in vegetation simulated by TRIFFID in that region are minor (Fig. 1). However, this contradicts data, which suggest a rather important reduction of tree cover in Amazonia at the LGM (Turcq et al. 2002). Is it therefore possible to use the present results to infer what could be the precipitation response if the sub-equatorial vegetation change was bigger? The scatter plot in Fig. 10, showing the vegetation-forced change in precipitation versus the change in tree fraction, suggests a fairly positive answer to that question. It is seen that the precipitation response to vegetation change is positively

correlated ($r = 0.6$) with the variation in tree fraction. A decrease in forest fraction by 10% corresponds to a decrease in precipitation by 21 mm/year. We recognise that some caution is needed when using linear regression: Zhang and Henderson-Sellers (1996), Eltahir (1996), Brovkin (2002) and Voldoire and Royer (2004) have, to various degrees and by different means, evidenced the possibly non-linear nature of the interactions between tropical forests and precipitation.

The analysis was repeated with LGM_VLGMT and LGM_VLGM289, and we found that the results of the linear regression are not statistically distinct to those obtained with LGM_VLGM, which has two implications. First, it confirms our analysis that the precipitation response to vegetation changes above the tropical rainforest is related to regional mechanisms. Indeed, if the tropical precipitation response had been remotely forced, a significant difference would have been observed in the regression and correlation coefficients obtained with LGM_VLGM and LGM_VLGMT. Secondly, the magnitude of this response is related to the structural changes in vegetation. The effect of stomatal opening, estimated by comparing LGM_VLGM289 with LGM_VLGM, cannot be distinguished statistically. This latter finding reinforces those by Crowley and Baum (1997), and Levis et al. (1999) who reached similar conclusions by means of different experimental designs. As already emphasised by Crowley and Baum (1997), this result is useful because simulations of the LGM participating to inter-comparison exercises do not always use the same concentration of $CO_2$ in plant physiology equations.

## 6 Conclusion

We have undertaken a series of climate simulations of the LGM performed with the atmosphere-mixed layer slab model HadSM3, to test the sensitivity of the climate to various changes in vegetation. Five questions were raised in the introduction, which we answer below.

1. *What are the impacts of vegetation changes between the pre-industrial epoch and the LGM on the energy balance of the system*? The disappearance of vegetation in Siberia and in Tibet produces, through a positive feedback loop involving vegetation, snow-cover and temperature, an important cooling of the surface compatible with previous estimates. The global, annual mean, clear-sky surface short-wave forcing is $-1.4$ W/m$^2$, and the effect on global, annual mean temperature, is an additional cooling of 0.6°C. The partial disappearance of vegetation in the tropics has a significant, but fairly small, negative impact on the turbulent exchanges of sensible heat (in semi-arid areas) and latent heat (in tropical rainforest areas).
2. *What are the consequences for atmosphere dynamics*? In summer, the coolings over Siberia and Tibet cause a southward shift of the sub-tropical front. This re-

duces the intensity of the tropical easterly jet which, because of momentum conservation, slows down the low-level monsoon circulation. This, in turn, alters the low-level transport of moisture, resulting in an increase in precipitation around northern Australia, and a decrease in convective precipitation east of Indonesia. In addition, changes in vegetation may have a regional impact on the intensity or the frequency of convective events. This is seen, in our model, in Africa and the south-west of Tibet.
3. *Can vegetation changes in one location influence climate (and perhaps vegetation) somewhere else*? The Arctic cooling is enhanced when global vegetation changes are taken into account. Furthermore, the disappearance of trees in Russia reinforces the cooling caused by local vegetation changes in Tibet. Because of the specific configuration of summer monsoon at the LGM simulated by this model, the weakening of the summer tropical easterly jet did not produce sizeable changes in continental rainfall. Therefore, high-latitude vegetation changes influenced the tropical climate, but it cannot be argued that they impacted tropical vegetation.
4. *Can we infer general conclusions about the impact of changes in tropical rainforest on climate*? There is a positive correlation between the variation in tree fraction and the resulting change in precipitation, with a slope of 2.1 mm/year/percent of tree-cover. There is thus a positive feedback between changes in rainforest and precipitation, as in previously published simulations. It was also seen that the effect of stomatal opening on precipitation is negligible. In the PMIP and MOTIF model-data inter-comparison projects, different models will use different vegetation boundary conditions for the LGM, depending on their vegetation components. Presenting results by means of scatter plots provides a useful complement to compare models and assess their performance.
5. *How will our results guide us in future experiment designs and analyses*? The present study underlines that a carefully validated representation of snow field albedo is important to quantitatively estimate the feedback of vegetation on climate. Further analysis of modern data are probably needed to more accurately document the snow field albedo as a function of the underlying surface type. Our study has also demonstrated that vegetation change in one location may potentially affect climate several thousands of kilometres away. However, this remote action may be conditioned by threshold phenomena, such as the settlement of perennial snow in Tibet. Therefore, multi-model ensembles are needed for truly robust inferences, and we hope the PMIP and MOTIF projects will investigate these issues further.

# References

Bamzai AS, Marx L (2000) COLA AGCM simulation of the effect of anomalous spring snow over Eurasia on the Indian summer monsoon. Q J R Meteorol Soc 126:2575–2584

Barnett TP, Dumenil L, Schlese U, Roeckner E (1989) The effect of Eurasian snow cover on regional and global climate variations. J Atmos Sci 46:661–685

Becker BD, Slingo JM, Ferranti L, Molteni F (2001) Seasonal predictability of the Indian Summer Monsoon: what role do land surface conditions play? Mausam 52:175–190

Berger A (1978) Long-term variations of daily insolation and quaternary climatic changes. J Atmos Sci 35:2362–2367

Berger A (2001) The role of $CO_2$, sea-level and vegetation during the Milankovitch-forced glacial-interglacial cycles. In: Proceedings "Geosphere-Biosphere Interactions and Climate". Cambridge University Press, New York, pp 119–146

Blanford HF (1884) On the connexion of the Himalayan snowfall with dry winds and seasons of droughts in India. Proc R Soc Lond 37:3–22

Bonan GB, Pollard D, Thompson SL (1992) Effects of boreal forest vegetation on global climate. Nature 359:716–718

Brovkin V (2002) Climate–vegetation interactions. J Phys IV PR 10:57–72

Bush ABG (2002) A comparison of simulated monsoon circulations and snow accumulation in Asia during the mid-Holocene and at the Last Glacial Maximum. Global Planet Change 32:331–347

Cox PM, Huntingford C, Harding RJ (1998) A canopy conductance and photosynthesis model for use in a GCM land surface scheme. J Hydrol 212–213:79–94

Cox PM, Betts RA, Bunton CB, Essery RLH, Rowntree PR, Smith J (1999) The impact of new land surface physics on the GCM simulation of climate and climate sensitivity. Clim Dyn 15:183–203

Cox PM, Betts RA, Jones CD, Spall SA, Totterdell IJ (2001) Modelling vegetation and the carbon cycle as interactive elements of the climate system. In: Pearce R (ed) Meteorology at the millennium. Academic, New York, pp 259–279

Crowley T, Baum S (1997) Effect of vegetation on an ice-age climate model simulation. J Geophys Res 102(D14):16463–16480

Crucifix M, Loutre MF (2002) Transient simulations over the last interglacial period (126–115 kyr bp): feedback and forcing analysis. Clim Dyn 19:419–433

Crucifix M, Betts RA, Cox PM (2005b) Vegetation and climate variability: a GCM modelling study. Clim Dyn 24:457–467 DOI 10.1007/s00382-004-0504-z

Crucifix M, Betts RA, Hewitt CD (2005a) Pre-industrial-potential and last glacial maximum global vegetation simulated with a coupled climate-biosphere model: diagnosis of bioclimatic relationships. Global and Planet Change 45:295–312 DOI 10.1016/j.gloplacha.2004.10.001

Dickson RR (1984) Eurasian snow cover versus Indian monsoon rainfall—an extension of the Hahn-Shulka results. Q J R Meteorol Soc 23:171–173

Eltahir EAB (1996) Role of vegetation in sustaining large-scale atmospheric circulation in the tropics. J Geophys Res 101(D2):4255–4268

Essery RLH, Best MJ, Betts RA, Cox PM, Taylor CM (2003) Explicit representation of subgrid heterogeneity in a GCM land-surface scheme. J Hydrometeorol 4(3):530–543

Ganopolski A, Rahmstorf S, Petoukhov V, Claussen M (1998) Simulation of modern and glacial climates with a coupled global model of intermediate complexity. Nature 391:351–356

Hahn D, Shukla J (1976) An apparent relationship between Eurasian snow cover and Indian monsoon rainfall. J Clim 33:2461–2462 DOI 10.1175/1520–0469

Harrison SP, Braconnot P, Joussaume S, Hewitt CD, Stouffer RJ (2002) Comparison of palaeoclimate simulations enhances confidence in models. EOS Trans Am Geophys Union 83:447

Harvey LDD (1988) On the role of high latitude ice, snow and vegetations feedbacks in the climatic response to external forcing changes. Clim Change 13:191–224

Hewitt CD, Senior CA, Mitchell JFB (2001) The impact of dynamic sea-ice on the climatology and climate sensitivity of a GCM: a study of past, present, and future climates. Clim Dyn 17:655–668

Hewitt CD, Stouffer RJ, Broccoli AJ, Mitchell JFB, Valdes PJ (2003) The effect of ocean dynamics in a coupled GCM simulation of the last glacial maximum. Clim Dyn 20:203–218 DOI 10.1007/s00382-002-0272-6

Inness PM, Slingo JM, Woolnough SJ, Neale RB, Pope VD (2001) Organization of tropical convection in a GCM with varying vertical resolution; implications of the Madden-Julian Oscillation. Clim Dyn 17:777–793

Kubatzki C, Claussen M (1998) Simulation of the global bio-geophysical interactions during the Last Glacial maximum. Clim Dyn 14:461–471

Levis S, Foley JA, Pollard D (1999) CO2, climate, and vegetation feedbacks at the Last Glacial Maximum. J Geophys Res 104(D24):31191–31198

Otterman J, Chou MD, Arking A (1984) Effects of nontropical forest cover on climate. J Appl Meteorol 23:762–767

Peltier WR (1994) Ice age paleotopography. Science 265:195–201

Pope VD, Stratton RA (2002) The processes governing horizontal resolution sensitivity in a climate model. Clim Dyn 19:211–236

Pope VD, Gallani ML, Rowntree PR, Stratton RA (2000) The impact of new physical parametrizations in the Hadley Centre climate model—HadAM3. Clim Dyn 16:123–146

Rayner NA, Horton EB, Parker DE, Folland CK, Hackett RB (1996) Version 2.2 of the global sea-ice and sea surface temperature data set, 1903–1994. CRTN74, Hadley Centre for Climate Prediction and Research Met Office, Bracknell, RG12 2SY

Rodwell MJ, Hoskins BJ (2001) Subtropical anticyclones and summer monsoons. J Clim 14:3192–3211

Turcq B, Cordeiro RC, Sifeddine A, Simoes FFL, Albuquerque ALS, Abrao JJ (2002) Carbon storage in Amazonia during the Last Glacial Maximum: secondary data and uncertainties. Chemosphere 49(8):821–835

Vernekar AD, Zhou J, Shukla J (1995) The effect of Eurasian snow cover on the Indian monsoon. J Clim 8:248–266

Viterbo P, Betts AK (1999) Impact on ECMWF forecasts of changes to the albedo of the boreal forests in the presence of snow. J Geophys Res 104:27803–27810

Voldoire A, Royer JF (2004) Tropical deforestation and climate variability. Clim Dyn 22:857–874 DOI 10.1007/s00382-004-0423-z

Wilson MF, Henderson-Sellers A (1985) A global archive of land cover and soils data for use in general circulation climate models. J Climatol 5:119–143

Wyputta U, McAvaney BJ (2001) Influence of vegetation changes during the Last Glacial Maximum using the BMRC atmospheric general circulation model. Clim Dyn 17:923–932

Xue Y, Shukla J (1996) The influence of land surface properties on Sahel climate. Part II: afforestation. J Clim 9:3260–3275

Yasunari T, Kitoh A, Tokioka T (1991) Local and remote responses to excessive snow mass over Eurasia appearing in the northern spring and summer climate—a study of the MRI GCM. J Meteorol Soc Jpn 69:473–487

Zhang H, Henderson-Sellers A (1996) Impacts of tropical deforestation. Part I: process analysis of local climatic change. J Clim 9:1497–1517

Zhang YS, Li T, Wang B (2004) Decadal change of the spring snow depth over the Tibetan Plateau: the associated circulation and influence on the East Asian summer monsoon. J Clim 17(14):2780–2793